Letters

An Improved Variable On-Time Control Strategy for a CRM Flyback PFC Converter

Chengdong Zhao, *Student Member, IEEE*, Junming Zhang, *Senior Member, IEEE*, and Xinke Wu, *Member, IEEE*

***Abstract*—The traditional critical conduction mode (CRM) flyback PFC converter with constant on-time control strategy usually suffers low power factor (PF) and high total harmonic distortion (THD) due to the nonsinusoidal input current waveform. In order to solve this problem, an improved variable on-time control strategy for the CRM flyback PFC converter is proposed in this letter. A simple analog divider circuit consisting of an operational amplifier, two signal switches, and an *RC* filter is proposed to modulate the turn-on time of the primary switch, and the PF and THD of the CRM flyback PFC converter can be evidently improved. The theoretical analysis is presented and the experiment results verify the advantages of the proposed control scheme.**

***Index Terms*—Critical conduction mode (CRM), flyback converter, power factor correction (PFC), variable on time (VOT).**

I. Introduction

At present, most ac/dc converters are forced to reduce the harmonic current to meet the power factor (PF) and harmonic current requirements, such as IEC61000-3-2, energy star specifications, and DesignLights Consortium [1]–[3]. As a result, active PFC converters have been widely used in both low-power and high-power applications [4], [5].

In low-power applications, the flybak power factor correction (PFC) converter operating in critical conduction mode (CRM) is widely used for the advantages of input and output isolation capability, simple structure, and low cost [6]–[8]. The major benefit of the CRM flyback PFC converter, compared to CCM flyback PFC converter, is that zero-voltage turn-on for the primary power switch and zero-current turn-off for the secondary rectifier diode can be easily achieved [9], [10]. The most popular control scheme for CRM flyback PFC converter is constant on-time (COT) control scheme, and only a voltage control loop is needed [11]–[13]. The switch turns on for a predefined period and then turns off till the inductor current reaches zero. With COT control scheme, the input peak current automatically follows the input voltage in a line cycle. Generally, for COT-controlled boost PFC converter, the theoretical average input current is sinusoidal and the PF is unity. However, for a flyback PFC or a buck PFC converter, the average input current is also related to the duty cycle, which will lead to low PF and high THD. In some LED driver applications, the THD of LED driver should be below 20% as required by DesignLights Consortium [3], for LED lighting in India, the THD should be even below 15% [14]. Considering the variation in mass production, it is better to have THD less than 10% with universal input.

Literature [15] introduces a variable on-time (VOT) control scheme for CRM flyback PFC converter to improve its PF and THD performance. Although the theoretical PF is unity, the parameters should be very carefully designed and an extra multiplier is needed, which will increase the cost and control circuit complexity.

To further improve the performance of the CRM flyback PFC converter, this letter proposes an improved VOT control scheme by adding a simple and low-cost analog divider (consisting of an operational amplifier, two signal switches, and an *RC* filter) into the traditional COT control circuit. The circuit and parameters design are very simple. With the proposed control method, the input current is pure sinusoidal and unity PF can be achieved theoretically. In Section II, the operation principle of the proposed VOT control scheme is analyzed. The experimental results based on a 60-W prototype with universal ac input and 24-Vdc output is presented in Section III. Section IV concludes this letter.

II. Proposed VOT-Controlled CRM Flyback PFC Converter

A. Traditional COT-Controlled CRM Flyback PFC Converter

In this section, the traditional COT-controlled flyback PFC converter will be briefly reviewed. The main circuit and control diagram of a traditional COT-controlled flyback PFC converter are shown in Fig. 1(a), and the main operation waveforms during half a line cycle are shown in Fig. 1(b). In order to achieve COT, the bandwidth of the control loop should be quite narrow so as to maintain the voltage loop error signal $V_{\rm comp}$ almost constant during half a line cycle. In steady state, the peak current of the primary side can be expressed as

$$i_{L\_\rm peak}(t) = \frac{V_{\rm in}\sin(\omega t)}{L_m} \cdot T_{\rm on} \tag{1}$$

where $V_{\rm in}$ is the input peak voltage, L_m is the primary inductance of the flyback transformer, and $T_{\rm on}$ is the on-time of switch

Manuscript received June 2, 2016; revised July 3, 2016; accepted July 20, 2016. Date of publication July 27, 2016; date of current version November 11, 2016. This work was supported by the National Natural Science Foundation of China under Grants 51277161, 51522704, and 51477154, and by the Fundamental Research Funds for the Central Universities (2015XZZX004-27).

The authors are with the College of Electrical Engineering, Zhejiang University, Hangzhou 310027, China (e-mail: zhaocd@zju.edu.cn; zhangjm@zju.edu.cn; wuxinke@zju.edu.cn).

Color versions of one or more of the figures in this paper are available online at http://ieeexplore.ieee.org.

Digital Object Identifier 10.1109/TPEL.2016.2594201

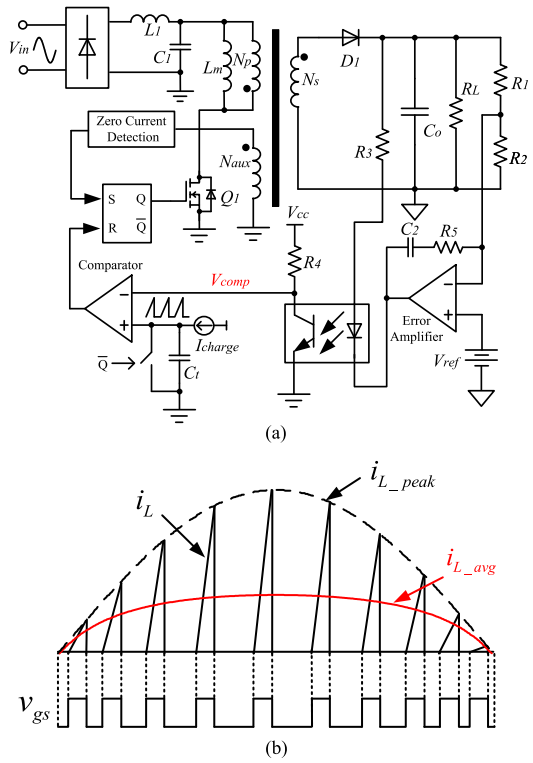

Fig. 1. Control scheme and theoretical waveforms of the traditional COT-controlled flyback PFC converter. (a) Control scheme. (b) Theoretical waveforms.

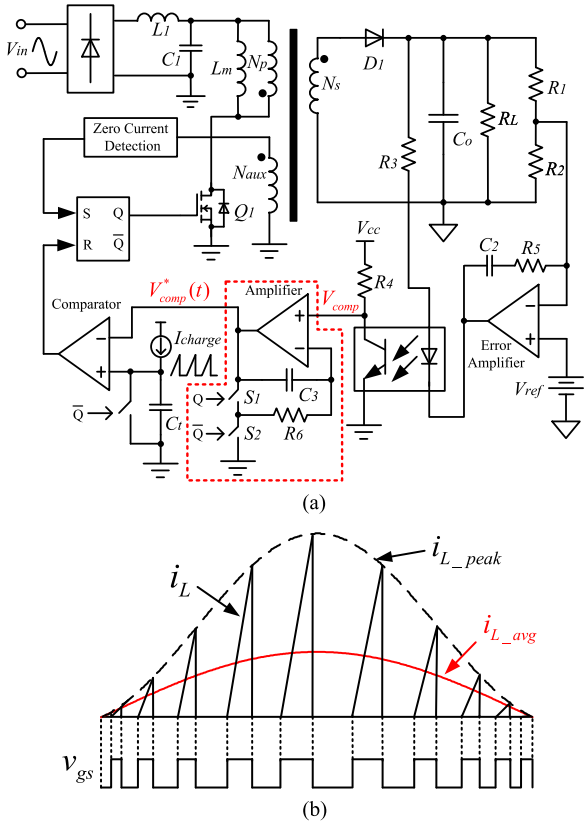

Fig. 2. Control scheme and theoretical waveforms of the proposed VOT-controlled flyback PFC converter. (a) Control scheme. (b) Theoretical waveforms.

Q_1, which is determined by the feedback loop error signal $V_{\rm comp}$ and keeps almost constant during half a line cycle.

Therefore, the average input current of primary side can be derived as

$$i_{L\_\rm avg}(t) = \frac{1}{2} i_{L\_\rm peak}(t) \cdot \frac{T_{\rm on}}{T_s(t)} = \frac{V_{in}\sin(\omega t) \cdot T_{\rm on} \cdot nV_o}{2L_m\left[V_{in}\sin(\omega t) + nV_o\right]} \tag{2}$$

where $T_s(t)$ is the switching cycle of primary switch Q_1, n is the transformer turns ratio (N_P/N_S), and V_o is the output voltage.

According to (2), the average input current $i_{L\_\rm avg}(t)$ is not sinusoidal, so the theoretical PF is not unity and the input current THD is high, especially when the reflected output voltage $n \cdot V_o$ is small and input voltage is high.

B. Proposed VOT-Controlled CRM Flyback PFC Converter

Fig. 2(a) shows the CRM flyback PFC converter with the proposed VOT control scheme. Only an extra analog divider (shown in red dash box) is required compared to the traditional COT control scheme. The structure of the analog divider is quite simple, which is consisted of an operational amplifier, two signal switches (S_1 and S_2) and an *RC* filter. S_1 and S_2 are only used for signal processing with very low voltage and current requirement, which can be implemented by standard analog switch like CD4053B, and the gate drive signal for Q_1 can be used as digital select signal. No extra driver circuit for S_1/S_2 is required. The two signal switches are complementarily controlled while the duty cycles of S_1 and S_2 are *d(t)* (the same as primary switch Q_1) and *1-d(t)*, respectively. R_6 and C_3 are used to filter out the switching frequency component and get a stable voltage at the inverting input terminal. The noninverting input voltage is $V_{\rm comp}$ from the output voltage feedback loop, the output of the operational amplifier is $V^*_{\rm comp}(t)$, and the average inverting input voltage is $V^*_{\rm comp}(t) \cdot d(t)$. In steady-state operation, the inverting input voltage of the operational amplifier follows the noninverting input voltage, so the output of the analog divider $V^*_{\rm comp}(t)$ equals to $V_{\rm comp}/{\rm d(t)}$, and the on-time of main switch Q_1 in the proposed method can be expressed as

$$T^*_{\rm on}(t) = \frac{C_t \cdot V^*_{\rm comp}(t)}{I_{\rm charge}} = \frac{C_t \cdot V_{\rm comp}}{I_{\rm charge} \cdot d(t)} = \frac{T_{\rm on}}{d(t)} \tag{3}$$

where

$$T_{\rm on} = \frac{C_t \cdot V_{\rm comp}}{I_{\rm charge}} \tag{4}$$

where C_t represents the timing capacitor and $I_{\rm charge}$ represents the controller internal charging current, as shown in Fig. 2(a). *d(t)* is the instant duty cycle of primary switch Q_1, and $V_{\rm comp}$ and $T_{\rm on}$ are constant like COT control.

According to (1), the average current of primary side can be also calculated as

$$i_{L\_\rm avg}(t) = \frac{1}{2} i_{L\_\rm peak}(t) \cdot d(t) = \frac{V_{in}\sin(\omega t)}{2L_m} \cdot T^*_{\rm on}(t) \cdot d(t). \tag{5}$$

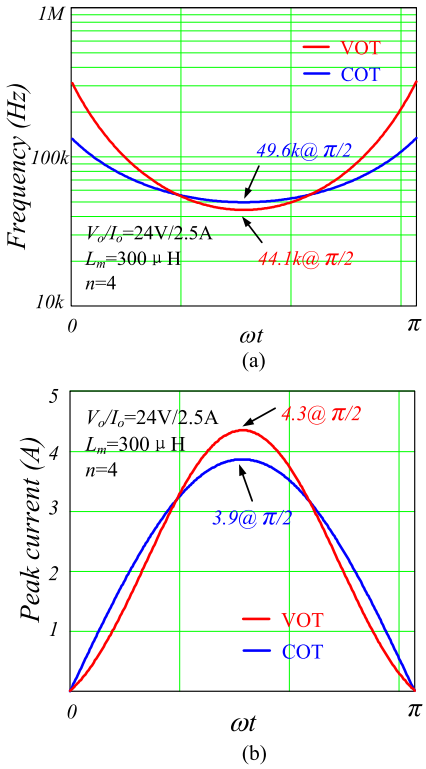

Fig. 3. Calculated switching frequency and inductor peak current at $V_{\rm in}$ = 110 V. (a) Switching frequency. (b) Inductor peak current.

Combining (3) and (5), the average input current can be derived as

$$i_{L\_\rm avg}(t) = \frac{V_{\rm in}\sin(\omega t)}{2L_m} \cdot T_{\rm on}. \tag{6}$$

According to (6), since $T_{\rm on}$ is constant as given in (4), the theoretical average input current of the proposed VOT-controlled flyback PFC converter is sinusoidal, which is not affected by the variation of the input voltage and output load. Hence, high PF and low THD can be achieved naturally.

Fig. 2(b) shows the theoretical waveforms of the flyback PFC converter with VOT control scheme. In order to achieve pure sinusoidal waveform for the average input current, the on-time of the primary switch is variable and the envelop of peak primary inductor current is no longer sinusoidal.

The proposed solution is a variable frequency control solution. Therefore, the design of the EMI filter is penalized in comparison to a fixed-frequency control solution, but it is the same as that with traditional COT control scheme. Generally, the design of the differential-mode (DM) filter is based on its minimum switching frequency, which can be obtained according to the noise at the critical frequency in the worst noise spectrum [16]. The calculated instant switching frequency and inductor peak current of both COT-controlled and VOT-controlled flyback PFC converter at 110-Vac input during half a line cycle are shown in Fig. 3. It can be seen that the VOT control scheme has a lower minimum switching frequency and higher maximum inductor peak current during half a line cycle, which indicates

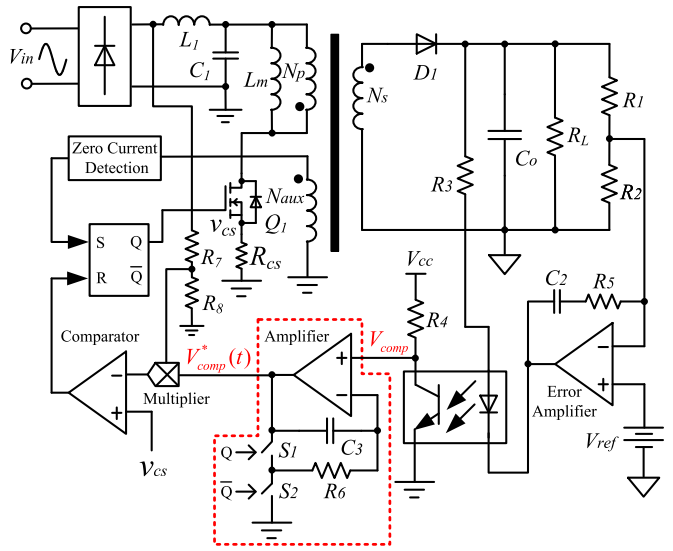

Fig. 4. Improved PCM-controlled CRM flyback PFC converter.

that a slightly larger DM filter is needed for VOT control scheme compared to COT control scheme.

C. Application in PCM-Controlled CRM Flyback PFC Converter

Another popular control scheme for the CRM flyabck PFC is peak current-mode (PCM) control method, which directly commands the peak input current following the input voltage waveform shape, such as L6562 from ST, and it has the same performance as the COT control scheme theoretically. The proposed analog divider can be also applied to the CRM flyback PFC converter with PCM control in the same way. Fig. 4 shows the proposed control scheme of the improved PCM flyback PFC converter. In steady state, the peak current of the primary side can be expressed as

$$\begin{aligned} i_{L\_\rm peak}(t) &= \frac{k \cdot V^*_{\rm comp}(t) \cdot V_{\rm in}\sin(\omega t)}{R_{cs}} \\ &= \frac{k \cdot V_{\rm comp} \cdot V_{in}\sin(\omega t)}{d(t) \cdot R_{\rm cs}} \end{aligned} \tag{7}$$

where k is a constant parameter represents the multiplier gain and input voltage waveform sensing gain, R_{cs} is the current sensing resistor.

So the average input current can be derived as

$$i_{L\_\rm avg}(t) = \frac{1}{2} \cdot i_{L\_\rm peak} \cdot d(t) = \frac{k \cdot V_{\rm comp} \cdot V_{\rm in}\sin(\omega t)}{2R_{\rm cs}}. \tag{8}$$

From (8), it can be seen that the average input current of the proposed PCM-controlled flyback PFC converter is also pure sinusoidal theoretically, and the theoretical waveforms are exactly the same as VOT-controlled flyback PFC converter as shown in Fig. 2(b). Therefore, in the experimental verification, only the results with the proposed VOT control scheme are presented.

TABLE I
KEY PARAMETERS OF THE PROTOTYPE

Parameters	Value
AC Input Voltage $V_{\rm ac}$	90–264 V
Output V_o / I_o	24 V/2.5 A
Primary Inductance of Transformer L_m	300 μH
Transformer Core	PQ26/25, PC40
Turns Ratio of Transformer $N_P : N_S : N_A$	40:10:5
Output Capacitor C_o	3000 μF/35 V
Main Switch Q_1	IPA60R160P6
Secondary Diode D_1	MUR820
DM Filter L_1 / C_1	350 μH/1 μF

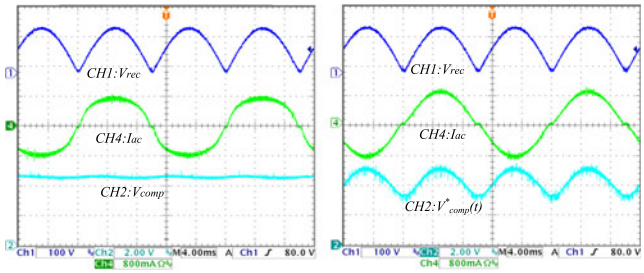

Fig. 5. Waveforms comparison with full load at 110-Vac input. (a) Traditional COT control scheme. (b) Proposed VOT control scheme.

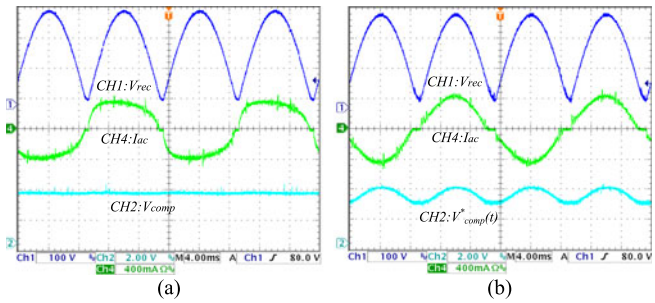

Fig. 6. Waveforms comparison with full load at 220-Vac input. (a) Traditional COT control scheme. (b) Proposed VOT control scheme.

III. EXPERIMENTAL VERIFICATION

A 60-W laboratory-made prototype with universal ac input and 24-Vdc output is built to verify the proposed VOT control scheme. The key parameters of the prototype are shown in Table I. As a comparison, a 60-W flyback PFC converter with the traditional COT control scheme is also built with the same parameters. The controller for traditional COT control is NCP1607, and the analog divider is implemented with LM358 and CD4053B (for S_1 and S_2).

The measured rectified input voltage $V_{\rm rec}$, input current $I_{\rm ac}$, and feedback loop error signal $V_{\rm comp}$ or $V^*_{\rm comp}(t)$ waveforms at 110- and 220-Vac inputs are shown in Figs. 5 and 6, respectively. It can be seen that the error signal $V_{\rm comp}$ for on-time control in traditional COT control scheme is constant, while the error signal $V^*_{\rm comp}(t)$ (output of the analog divider as shown in Fig. 2) for on-time control in the proposed VOT control scheme

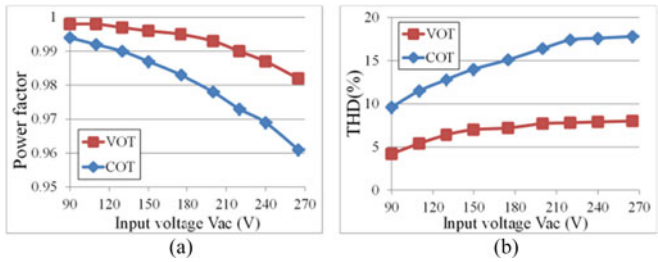

Fig. 7. PF and THD comparison at different input voltages. (a) PF comparison. (b) THD comparison.

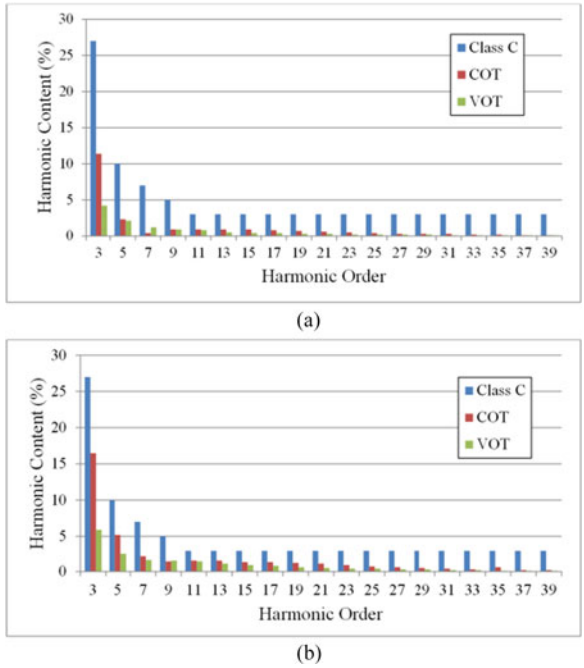

Fig. 8. Input current harmonics at 110- and 220-Vac inputs. (a) 110-Vac input. (b) 220-Vac input.

is no longer constant. As a result, the average input current is more sinusoidal than that of COT-controlled CRM flyback PFC converter during the whole input voltage range.

The PF and THD of COT-controlled and VOT-controlled flyback PFC converters at different input voltages and full load are shown in Fig. 7. From Fig. 7(a), it can be seen that the PF of VOT-controlled flyback PFC converter is always above 0.98 during the whole input range, which is always higher than that of COT-controlled flyback PFC converter.

The THD of VOT-controlled flyback PFC converter is well below 10% during the whole input range, which is much lower than that of COT-controlled flyback PFC converter from Fig. 7(b). The highest THD of VOT-controlled flyback PFC converter is 8.2% at 264-Vac input, while, the highest THD of COT-controlled PFC converter is 17.8% at 264-Vac input.

Fig. 8(a) and (b) shows the requirements of IEC61000-3-2 Class C and measured input current harmonic contents of COT-controlled and VOT-controlled flyback PFC converters at 110- and 220-Vac inputs, respectively. It can be seen that both COT and VOT control scheme can meet Class C limits, but the

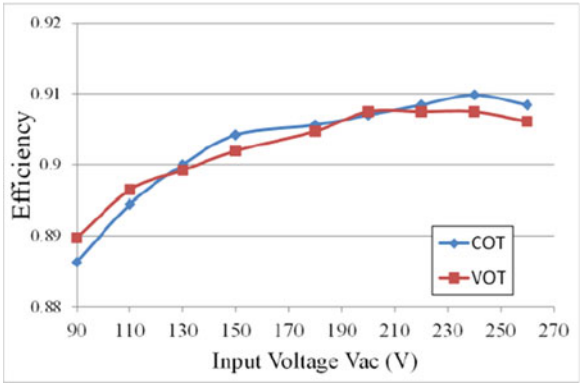

Fig. 9. Full load efficiency comparison at different input voltages.

proposed VOT-controlled flyback converter has much more margins than the traditional COT-controlled flyback PFC converter, especially the third and fifth harmonic contents.

Fig. 9 shows that the efficiencies of COT-controlled and VOT-controlled flyback PFC converter are almost the same.

IV. Conclusion

This letter presents a novel VOT control scheme to improve the PF and THD of CRM flyback PFC converter by adding a simple and low-cost analog divider circuit, which is consisted of an operational amplifier, two signal switches (S_1 and S_2) and an *RC* filter, and it can be easily integrated into the traditional PFC controller. The superiority of this method is its simplicity and great improvement of input current PF and THD compared to traditional COT-controlled CRM flyback PFC converter. Besides, the design of control circuit is much simpler compared to existing flyback VOT control scheme. The experimental results clearly verify the theoretical analysis.

References

[1] *Electromagnetic Compatibility (EMC)—Part 3-2: Limits—Limits for Harmonic Current Emissions (Equipment Input Current ≤ 16 A Per Phase)*, IEC International Standard 61000-3-2, 2005.

[2] Program Requirements for Solid State Lighting Luminaires, version 1.1, Energy Star, 2008.

[3] Technical Requirements Table, V4.0, DesignLights Consortium, 2016.

[4] J. Yang, J. Zhang, X. Wu, Z. Qian, and M. Xu, "Performance comparison between buck and boost CRM PFC converter," in *Proc. IEEE Control Model. Power Electron. Conf.*, Jun. 2010, pp. 1–5.

[5] M. M. Jovanovic' and Y. Jang, "State-of-the-art, single-phase, active power-factor-correction techniques for high-power applications—An overview," *IEEE Trans. Ind. Electron.*, vol. 52, no. 3, pp. 701–708, Jun. 2005.

[6] D. G. Lamar *et al.*, "Design-oriented analysis and performance evaluation of a low-cost high-brightness LED driver based on flyback power factor corrector," *IEEE Trans. Ind. Electron.*, vol. 60, no. 7, pp. 2614–2626, Jul. 2013.

[7] K.-W. Siu and Y.-S. Lee, "A novel high-efficiency flyback power-factor correction circuit with regenerative clamping and soft switching," *IEEE Trans. Circuit Syst. I, Fundam. Theory Appl.*, vol. 47, no. 3, pp. 350–356, Mar. 2000.

[8] J. Zhang, H. Zeng, and T. Jiang, "A primary-side control scheme for high power-factor LED driver with TRIAC dimming capability," *IEEE Trans. Power Electron.*, vol. 27, no. 11, pp. 4619–4629, Nov. 2012.

[9] X. Wu, J. Yang, J. Zhang, and Z. Qian, "Variable on-time (VOT)-controlled critical conduction mode buck PFC converter for high-input ac/dc HB-LED lighting applications," *IEEE Trans. Power Electron.*, vol. 27, no. 11, pp. 4530–4539, Nov. 2012.

[10] J. S. Lai and D. Chen, "Design consideration for power factor correction boost converter operating at the boundary of continuous conduction mode and discontinuous conduction mode," in *Proc. IEEE Appl. Power Electron. Conf. Expo.*, Mar. 1993, pp. 267–273.

[11] J. J. Zheng, A. Shteynberg, D. Zhou, and J. McCreary, "A novel multimode digital control approach for single-stage flyback power supplies with power factor correction and fast output voltage regulation," in *Proc. IEEE Appl. Power Electron. Conf.*, Mar. 2005, pp. 830–836.

[12] J. Yang, J. Zhang, X. Wu, Z. Qian, and M. Xu, "Performance comparison between buck and boost CRM PFC converter," in *Proc. IEEE 12th Workshop Control Modeling Power Electron.*, 2010, pp. 1–5.

[13] X. Wu, J. Yang, J. Zhang, and M. Xu, "Design considerations of soft switched buck PFC converter with constant on-time (COT) control," *IEEE Trans. Power Electron.*, vol. 26, no. 11, pp. 3144–3152, Oct. 2011.

[14] 2015. [Online]. Available: www.eeslindia.org/writereaddata/Section 4 Technical and SCC.pdf

[15] T. Yan, J. Xu, F. Zhang, J. Sha, and Z. Dong, "Variable-on-time-controlled critical-conduction-mode flyback PFC converter," *IEEE Trans. Ind. Electron.*, vol. 61, no. 11, pp. 6091–6099, Nov. 2014.

[16] F Yang, X. Ruan, Q. Ji, and Z.H. Ye, "Input differential-mode EMI of CRM boost PFC converter," *IEEE Trans. Power Electron.*, vol. 28, no. 3, pp. 1177–1188, Mar. 2013.